

# **The Seamount Effect: an Empirical Characterization and Visualization of Winslow Reef, a Seamount in PIPA**

S261 Protecting the Phoenix Islands

Directed Oceanographic Research

Samuel Hill, Nathan Kemp, Karl Kiser, Emily Sage Landers, and Christina Quinn

## **Abstract:**

Within the Phoenix Islands Protected Area (PIPA) are many seamounts, submerged mountains, which have a noticeable impact on the current flow and other biological and physical characteristics of the surrounding water. The study uses data collected in and around Winslow Reef, a seamount in PIPA, and assess the parameters of current flow, salinity levels, chlorophyll a concentrations, and zooplankton density for the seamount area. An assessment of the potentiality of seamounts to be hotspots of biodiversity/biomass, as well as their display of the Island Mass Effect (IME) was carried out; the data collected supports that Winslow displays specific changes in the primary and secondary productivity levels, and has characteristics descriptive of the IME.

## **Introduction:**

The Phoenix Island Protected Area (PIPA) is a Marine Protected Area (MPA) that is chiefly open water, with seamounts and atolls providing the dominant geological features. A seamount is characterized as an underwater mountain generated by volcanic activity whose summit sits 1000 m or less below the sea surface (Pitcher et al. 2007). In PIPA, they have been largely overlooked in terms of their possibilities as hotspots for productivity and biodiversity and thusly as key areas to protect (Morato et al., 2010a) – especially for pelagic and commercially important fisheries such as tuna (Morato et al. 2010b). This is due in part to their terrestrial cousins, the atoll. These atolls, ‘islands’, have land resources that are considered valuable as well as various effects on the surrounding water column. The major effect to note is the Island Mass Effect (IME), which is a theory that describes what happens when you place a large mass in the middle of a flowing body of water. Physically, this is thought to create diversion of currents and turbulence, complex patterns of water flow such as eddies and circulation (e.g. Taylor Cones), and disruptions in nutricline stratification - i.e. upwelling (Bakun, 1986; Boehlert and Genin, 1987; Pennington et al., 2006). It is also theorized that a result of these physical phenomena is relatively higher densities of primary and secondary productivity (Gilmartin and Revelante, 1974; Hernández-León, 1991). However, IME is to some degree a misnomer as this effect is also a significant characteristic of seamounts as they provide “enhanced hydrodynamic activity compared to the flat abyssal ocean” (Pitcher et al. 2007). It would be foolish then to ignore these geologic behemoths because of their lack of a surface profile; these underwater mountains change the physical parameters within the water column and are biological hotspots.

Some estimates exceed a million seamounts worldwide, but the locations have been traditionally difficult to pin down. The advent of satellite remote sensing has made the world of seamounts exponentially more accessible. Some researchers have used remote sensing to analyze the mean and total chlorophyll a (Chl a) concentrations as well as total sea surface temperature (Elliot et. al, 2012). This was then spatially cross-correlated with satellite images to determine what type of relationships existed near or away from reefs in the study site. Other groups have

used technologies such as the Regional Ocean Modeling System (a primitive equations ocean model) along with high-resolution data sets to reveal the significant impact of small islands on a comparatively massive biological bloom (Messie et. al. 2006). Their results suggested that the small Kiribati islands were partially responsible for the local perturbations of the large-scale equatorial dynamics specific to the El Nino/La Nina transition period, and were therefore responsible for the location and intensity of the bloom. Some have used satellite data to analyze Chl a, sea surface height anomaly, temperature, wind, and rainfall to show the seasonality of phytoplankton blooms around the Marquesas Islands (Martinez and Maamaatuaiahutapu, 2004). They found three types of blooms: seasonal, episodic, and La Nina-related. The initiation of these blooms is due to the IME and different kinds of blooms can be explained by the dynamic interaction of circulation and topography. The IME blooms are correlated with the total surface current and episodically correlated with the geostrophic current. In modeled seamounts of the Northeast Atlantic, large aggregations of fish have been found, supporting the idea that different seamounts may potentially be hotspots of biodiversity or biomass (Morato et al., 2009). Due to the fact that phytoplankton and zooplankton make up a large portion of the biomass of Pacific regions, they are a good indicator of the productivity of an area.

The preceding research around seamounts seems heavily reliant on satellite imagery, existing ocean models, and continuous data sets from institutions like NOAA. While many researchers have used indirect technologies to measure the effects of seamounts on ocean characteristics and productivity, it is not common to have these effects measured directly. Although the various parameters that have been measured can help explain how the seamounts and islands affect the water column and productivity, the ground-truthing of the various models and satellite images is a crucial step towards a more secure understanding of the water column and productivity surrounding seamounts.

Our goal for this study is to characterize the physical parameters that make seamounts unique. Models based off of the characterization data collected during SEA Cruise S261 are created and used to further our understanding of biodiversity and productivity, and to see if the IME theory holds true. Consequently, this paper focuses on the physical characteristics of the water column around Winslow Reef – a single seamount in PIPA that has a very unique topography – and the resulting productivity of both phytoplankton and zooplankton. We expected to find that the currents are measurably and significantly disrupted by the seamounts, the physical parameters (namely temperature and salinity) will differ in relation to the currents, and levels of primary and secondary production will be different and higher near the seamount or downstream of it.

## **Methods:**

### 1: Collection

#### 1.1: Deployments and transects

The various forms of deployments were collected at specific stations and after stations at specific speeds for set amounts of times. The specific station deployments were for the Hydrocast Niskin Rosette (HC) and were at the following locations;

- 2°2.4'S, 174°14.6'W
- 1°41.9'S, 174°20.2'W

- 1°25.2'S, 174°30.1'W
- 1°38.3'S, 174°41.0'W
- 1°53.1'S, 174°54.5'W
- 1°24.7'S, 175°0.2'W
- 1°38.0'S, 175°6.8'W
- 1°51.9'S, 175°15.9'W

These specific stations fall along the transects at predetermined locations. After these stations, Tucker Trawls (TT) and Neuston Tows (NT) were carried out en route to the next station along our cruise track at set speeds. After the tows were completed, the towfin was deployed for the remainder of the course until reaching the next station. This allowed us to collect profile information along all of our transects. The transects were chosen to represent the up-current side, down-current side, as well as on and around the peaks of the seamount.

### 1.2: Hydrocast Niskin Rosette Deployments

The HC was lowered using a winch system to depths of 600m, with attached water collection bottles taking water samples at 600m, 500m, 400m, 300m, 250m, 200m, 150m, 125m, 100m, 75m, 50m, and 25m. A thirteenth bottle of surface water was also collected separately with our on board flow through system. Attached to the HC was a CTD (SBE19PlusV2, SeaBird Electronics, Bellvue, WA), sampling at a rate of 4 measurements/sec for temperature (°C) and salinity (psu) measurements. A flow through Seapoint fluourometer also attached to measure for Chl a (V).

### 1.3: Tucker Trawl Deployments

The TT deployments were done using a meter wide, 333 micron mesh net. They were towed at an approximate speed of 2 knots, being lowered up and down in the water column first to a goal depth of 50m (the deep tow), followed by two lowerings to 25m of depth (the shallow tows). The zooplankton densities collected from the TT are measured in mL/m<sup>3</sup>.

### 1.4: Neuston Net Deployments

The NT deployments were done using a meter wide, 333 micron mesh net. They were towed at the air water interface for 30 minutes, at an approximate speed of 2 knots. This was in an attempt to have 1 nautical mile (nm) of water pass through the net. The zooplankton densities collected from the NT are measured in mL/m<sup>2</sup>.

### 1.5: Towfin Deployments

The towfin was lowered on a winch to approximate depths of 200m, moving up and down the water column along sections of the SEA S261 course track (Figure 1). Attached to the towfin was an RBR CTD (Richard Branker Research Ltd (Ottawa, ON), XR-420 series) sampling at a rate of 1 measurement/sec for depth (m), temperature (°C), salinity (psu). As well, a Seapoint fluourometer sampling at a rate of 2 measurements/sec was attached to collect Fluourometric readings for Chl a concentrations (V).

### 1.6: En Route Collection

Equipped with acoustic instruments, we collected physical data continuously. With a 75kHz Array Ocean Acoustic Doppler Current Profiler (ADCP) (RD Instruments, San Diego, CA) we determined the horizontal current profile. Magnitude and direction of the horizontal current up to 600 meters was collected and analyzed. Bathymetric data was also collected while underway using a “Chirp”, Sub-bottom Profiler (3260, Knudsen Engineering Limited, Perth, Ontario, Canada).

## 2: Processing

### 2.1: Chlorophyll a concentrations

Water samples at goal depths of 0m, 25m, 50m, 75m, 100m, and 125m (collected from the HC deployments with an error range of approximately 0-1.6m off of goal depths) were analyzed for Chl a concentrations. The water was filtered through .45 micron filter paper and dissolved in acetone in the same manner as Parsons, Maita and Lilla (1989). These were then assessed for Chl a concentrations in ug/L. In order to convert the flourometer data (from either the HC flow through flourometer or the towfin sea-point fluorometer) into non-device dependent units, a linear regression was plotted. The regression used the discreet, extracted ug/L data from all 8 stations at the 6 depths analyzed, and compared them to the corresponding flourometer data for those depths (Figure 10). A line equation ( $[V] = 1.60488 * [ug/L] + .0320744$ ) was produced with an  $r^2$  value of .953747, and was then used to calibrate the flourometer data, converting the V measurements into ug/L.

### 2.2: Zooplankton density and diversity

Following each TT and NT deployment, matter collected by the nets was rinsed into buckets and processed according to standard Sea Education Association protocol. Nekton (including gelatinous organisms) > 2 cm in diameter and inorganic matter were first removed before the sample was filtered through a 333 micron mesh sieve. A 1.0 mL subsample, from which 100 organisms were randomly chosen and identified to the highest taxonomic resolution possible using a dissecting scope, was then collected from the bulk of the filtered sample. The biovolume of the remainder of the sample was determined via water displacement.

Zooplankton densities at each collection site were calculated based on the total biovolume of each sample collected, distances covered during each deployment and the known dimensions of the tucker trawl and neuston net mouths. Distances covered during each TT deployment were recorded via a flowmeter attached to the net, while distances covered during each NT deployment were measured using GPS positions recorded on a per-minute basis. Zooplankton diversity was determined by using data from the taxonomic assessments to calculate the Shannon Weiner Index.

## Results:

### Transects:

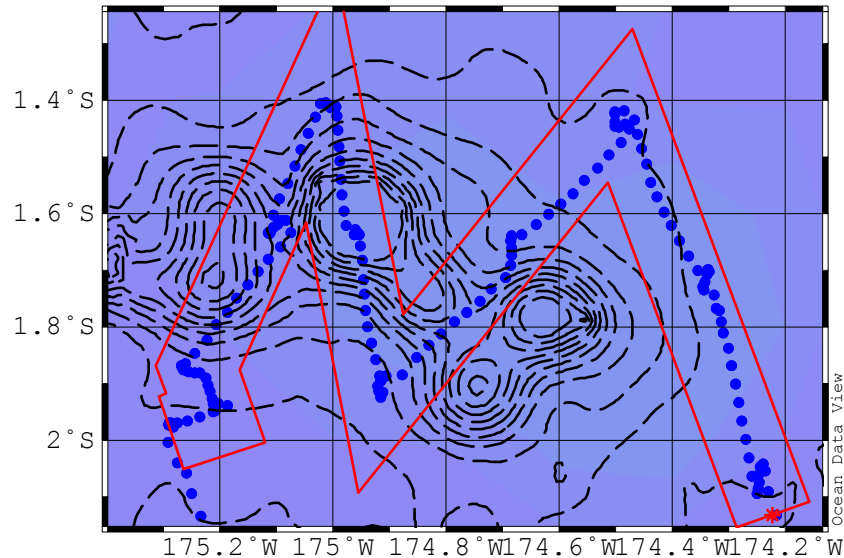


**Figure 1:** Transects of Winslow reef with the ADCP data plotted along the transects

### Currents:

The currents results encapsulate data retrieved from the ADCP while en route at the depths of 50m, 100m, 150m, and 200m (as these correlate with the salinity, Chl a, and zooplankton data). The flow lines indicate trends that we believe the raw current data exemplars and the labels of depth indicate peaks or channels based off of satellite topographical information obtaining using qGis or ground-truthed data collected via the “Chirp”.

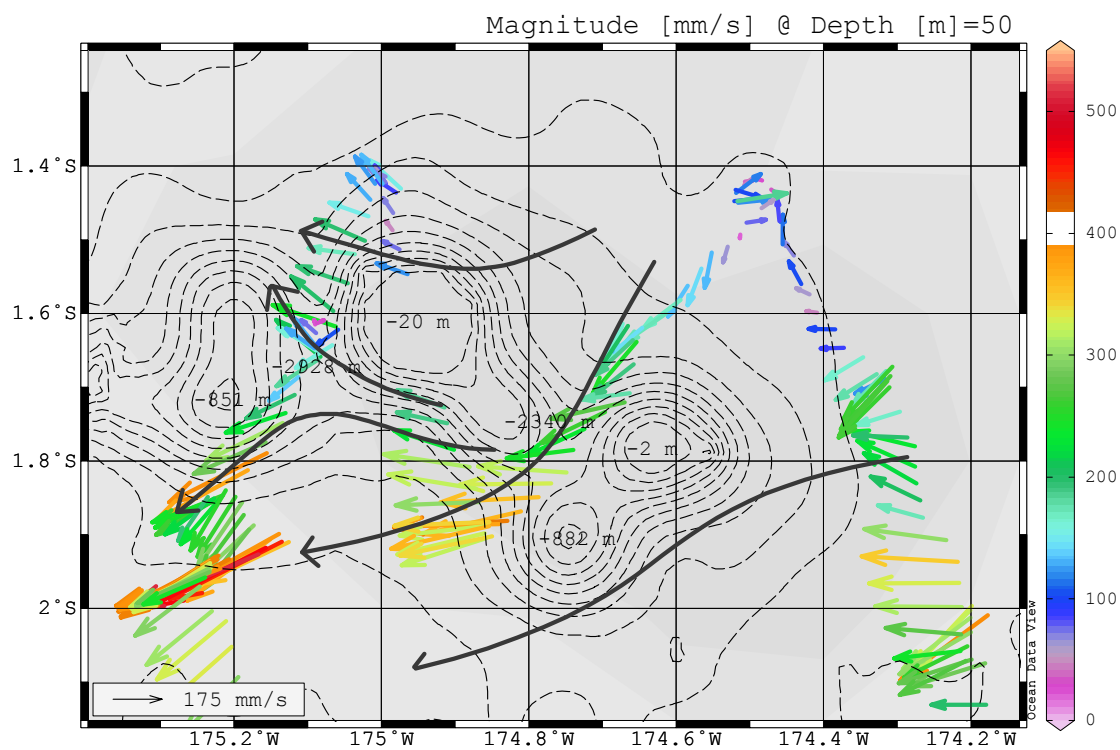


**Figure 2.** Current patterns at 50m

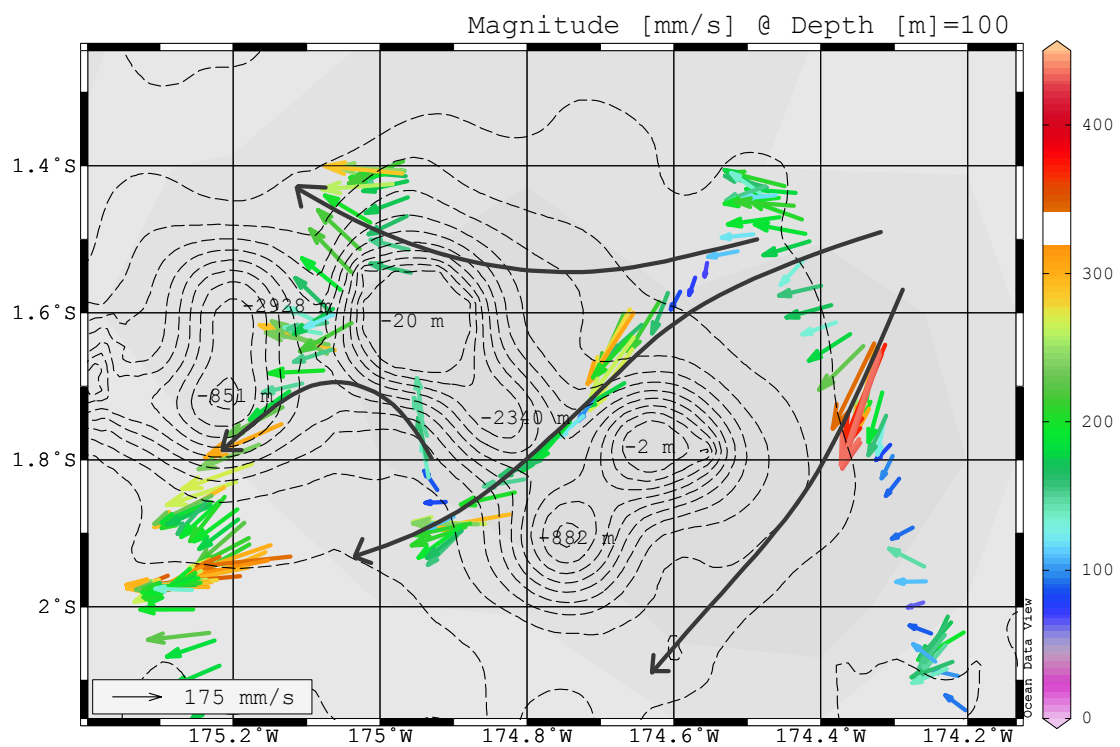


**Figure 3.** Current patterns at 100m

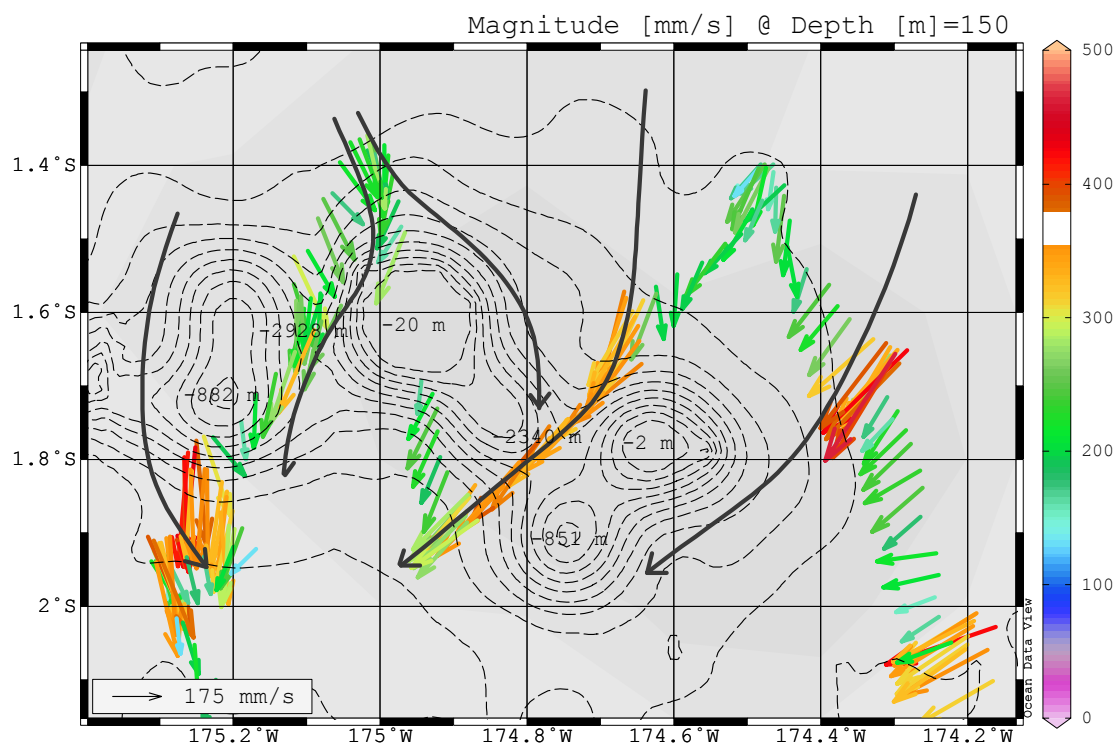


**Figure 4.** Current patterns at 150m

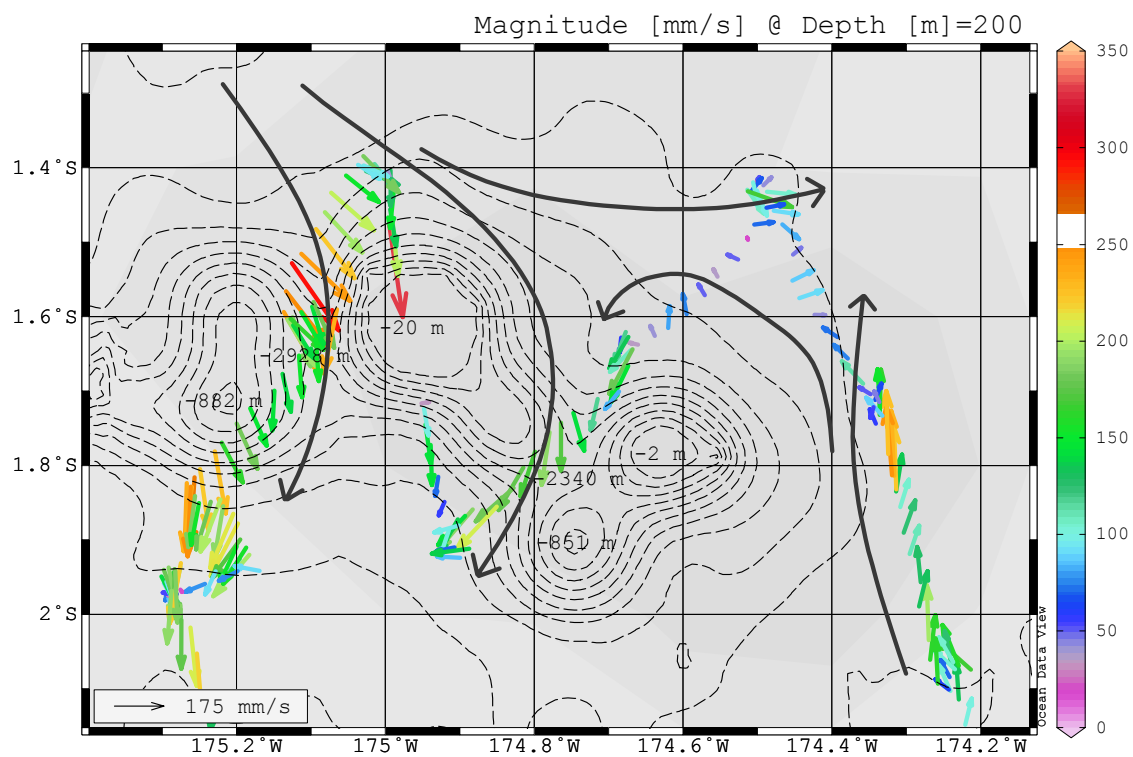


**Figure 5.** Current patterns at 200m

## Salinity:

The salinity results encapsulate data retrieved from CTD deployments and tows as we transected Winslow Reef from East to West, Starting in the South Eastern corner of the seamount. The transect represented in Figure 6 begins in the South Eastern most edge of Winslow and follows from South to North. The 34.75 isohaline line oscillates between 48m and 70m in depth and the mean depth gradually increases.

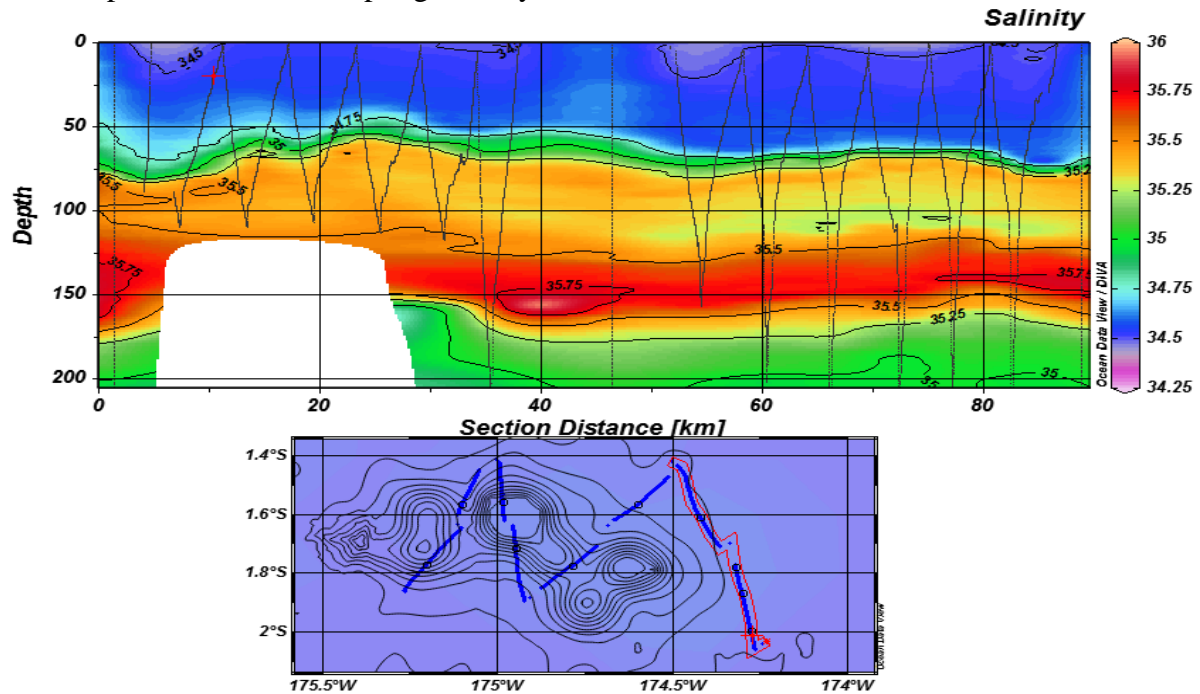


**Figure 6.** Salinity vs. Depth along the Eastern transect of Winslow.

The transect represented in Figure 7 begins in the North Easter edge of Winslow and follows from North to South. The 34.75 isohaline line oscillates between 50m and 65m in depth and the mean depth gradually decreases.



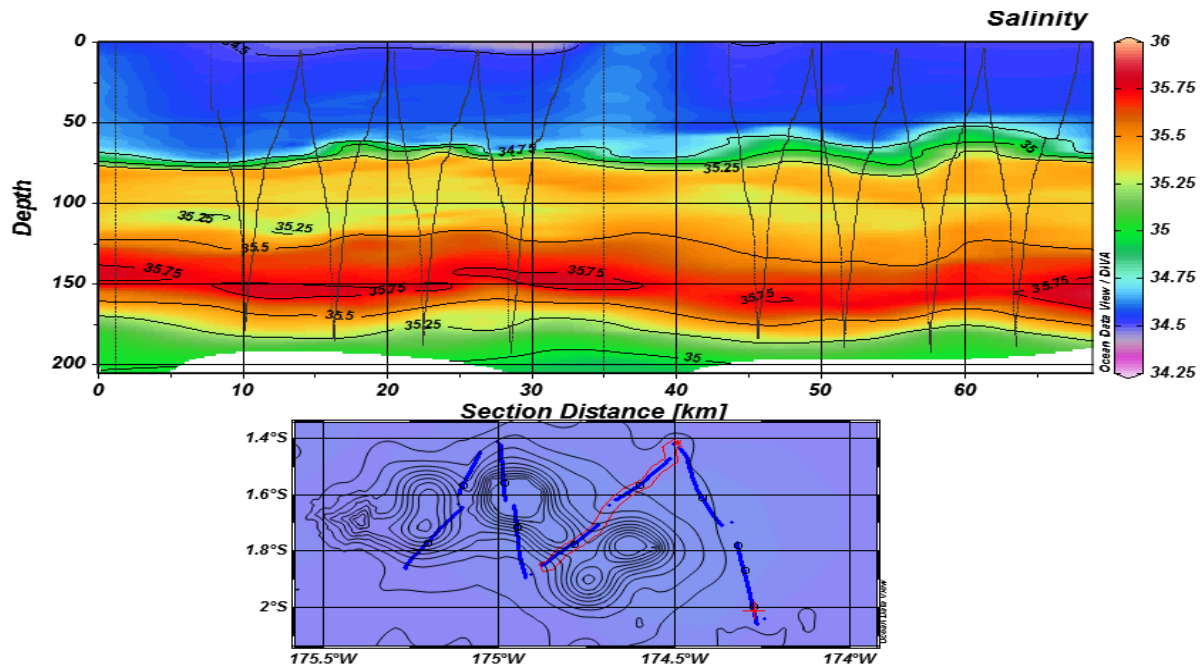


**Figure 7.** Salinity vs. Depth along the Central Eastern transect of Winslow.

The transect represented in Figure 8 begins in the Southern Central area of Winslow and follows from South to North. The 34.75 isohaline line oscillates between 48m and 55m in depth and the mean depth gradually increases.

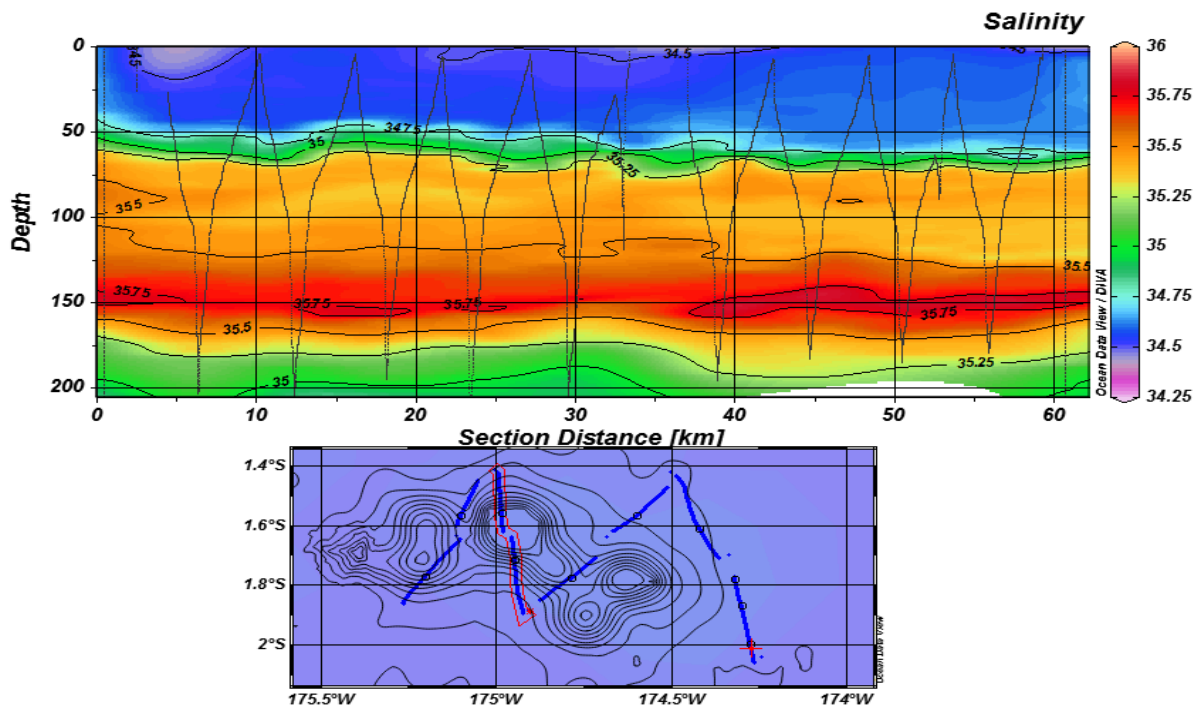


**Figure 8** Salinity vs. Depth along the Central Western transect of Winslow.

The transect represented in Figure 9 begins in the Northern Central area of Winslow and follows from North to south. The 34.75 isohaline line oscillates between 50m and 55m in depth and the mean depth gradually decreases.

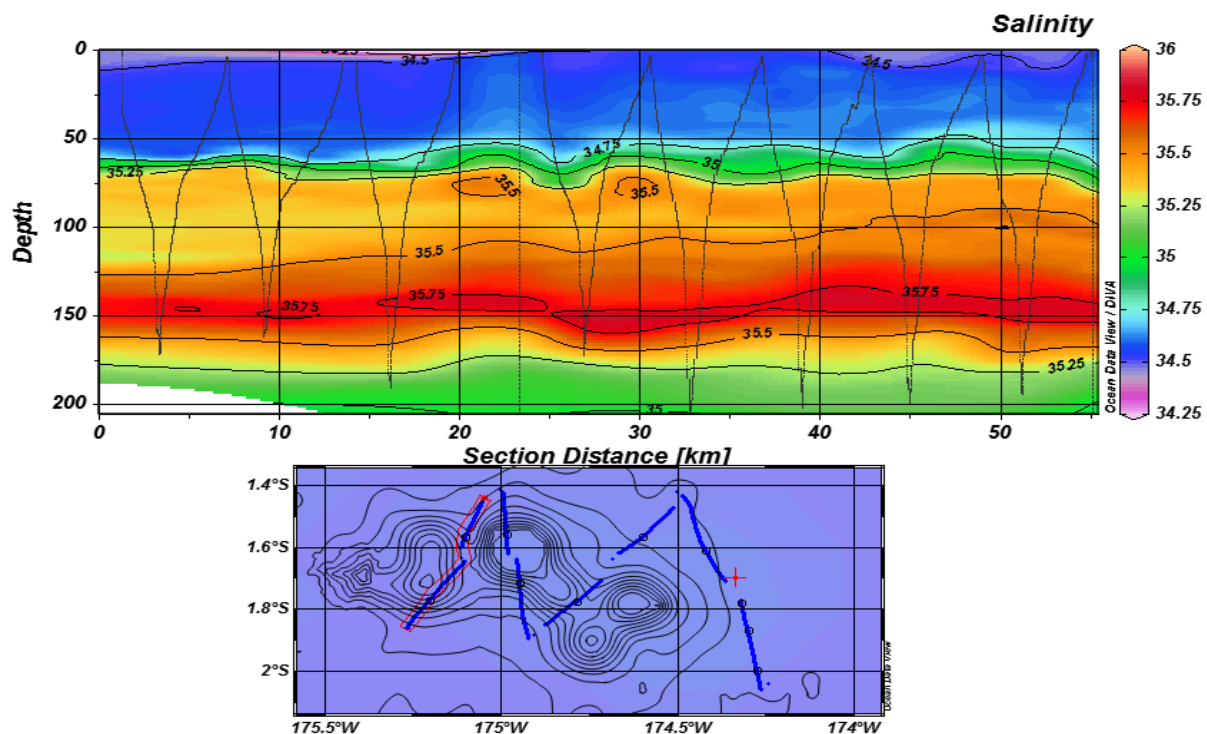


**Figure 9.** Salinity vs. Depth along the Western transect of Winslow.

#### Chlorophyll a:

The Chl a results encapsulate data retrieved from HC and towfin deployments as Winslow Reef was transected from East to West, starting in the South Eastern corner of the seamount area. Chl a concentrations are being used as a proxy for primary production in the Winslow area. Fluorometer data from both the HC and the towfin deployments were converted from V to ug/L using the equation presented in Figure 10.

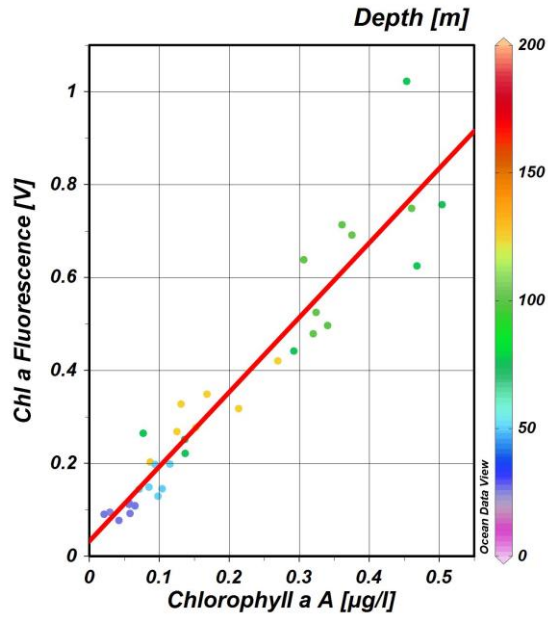


**Figure 10.** Linear regression comparing Chl a Fluorescence (V) to Chl a (ug/L) from all eight stations around Winslow Reef. Line equation: ( $[V] = 1.60488 * [ug/L] + .0320744$ ) with an  $r^2$  value of .953747.

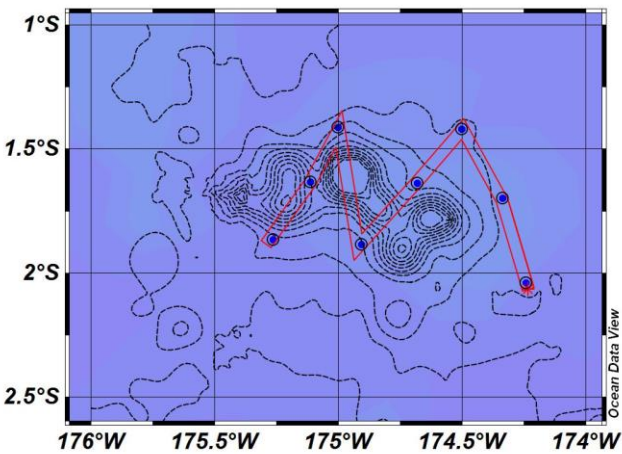


**Figure 11.** Locations of HC stations carried out around Winslow. The overlay depicts Winslow Reef bathymetry. The easternmost station was the first station completed.

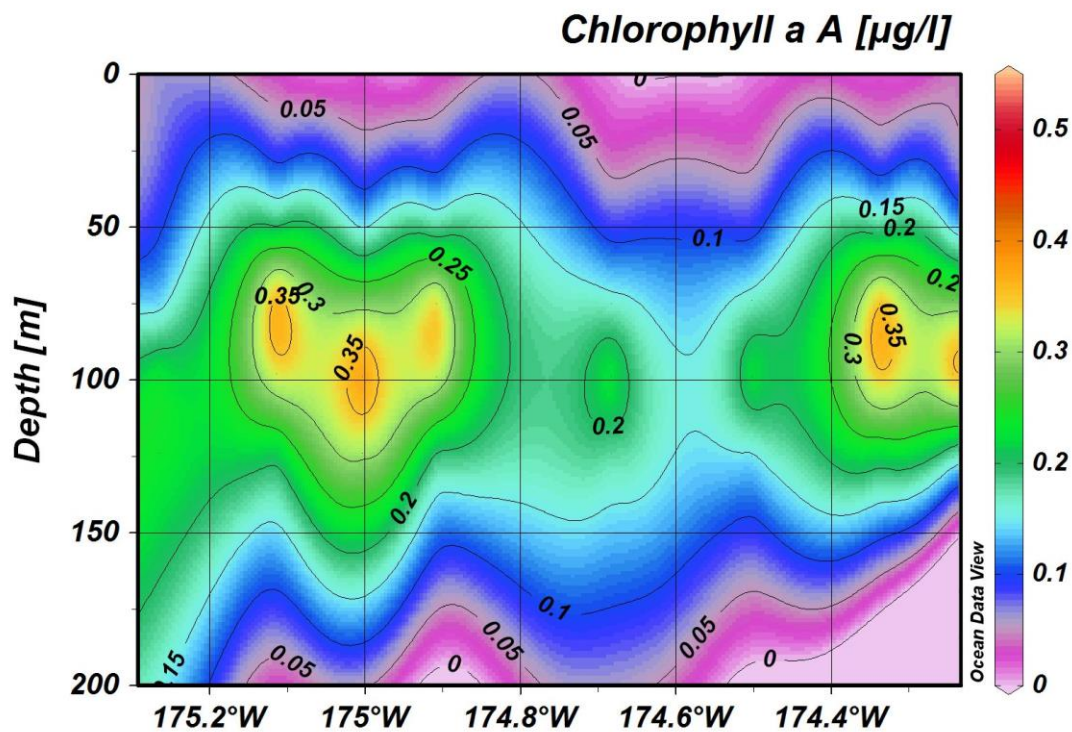


**Figure 12.** Grid plot of Chl a concentrations based off of HC extracted values. View depicts all eight station locations.

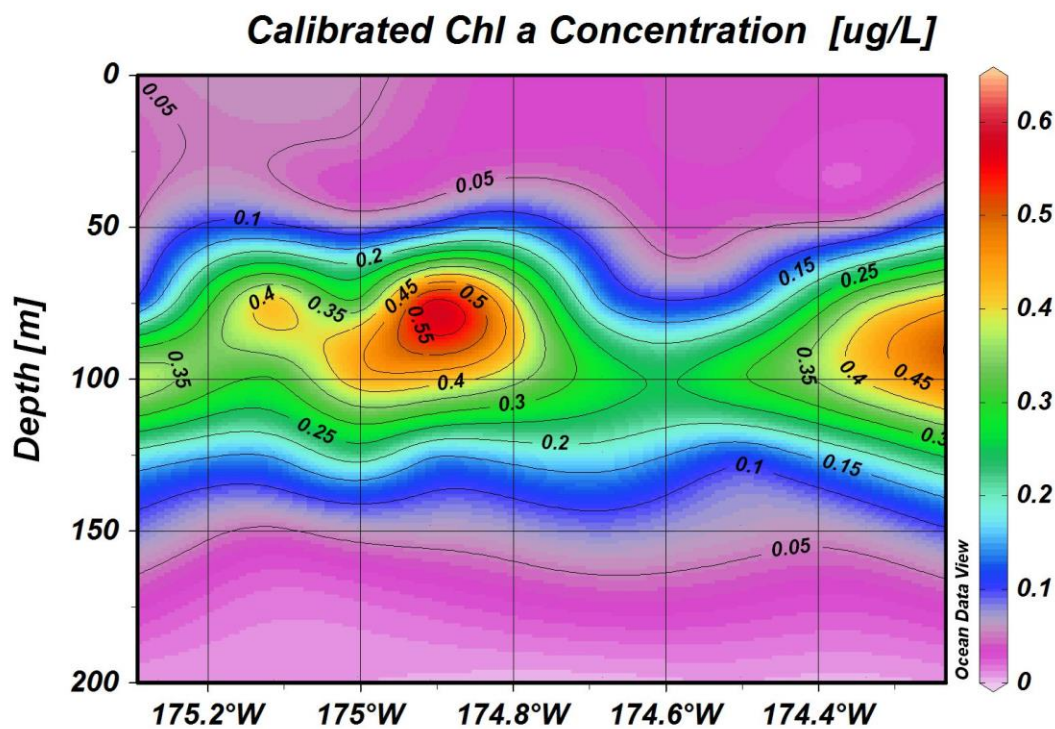


**Figure 13.** Grid plot of Chl a concentrations based off of Fluorometer data converted into  $\mu\text{g/L}$ . View depicts all eight station locations.



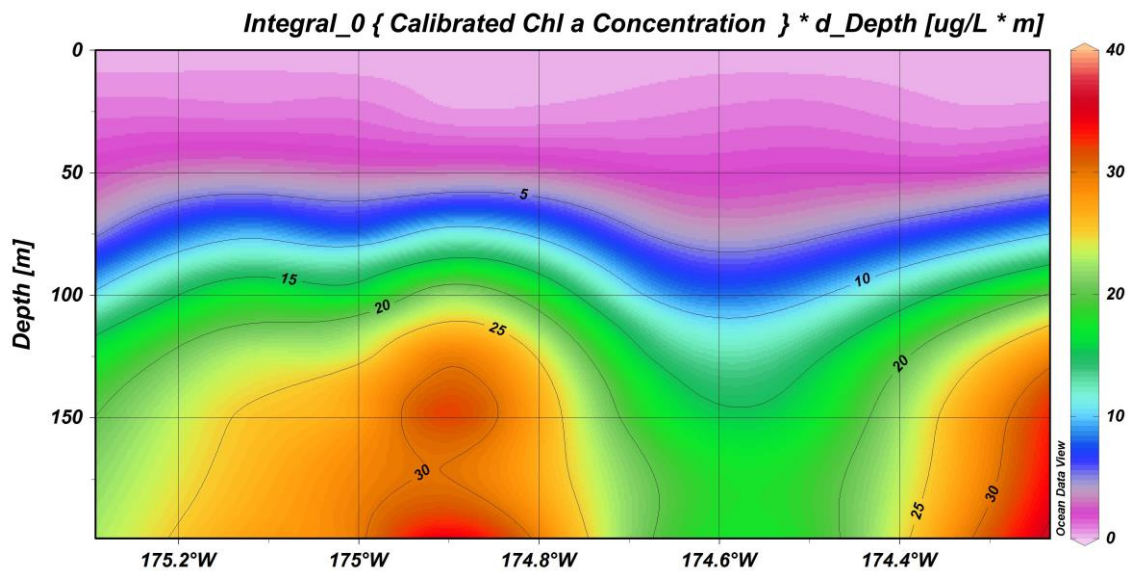


**Figure 14.** Cross sectional view of integrated Chl a concentrations. View depicts all eight station locations.

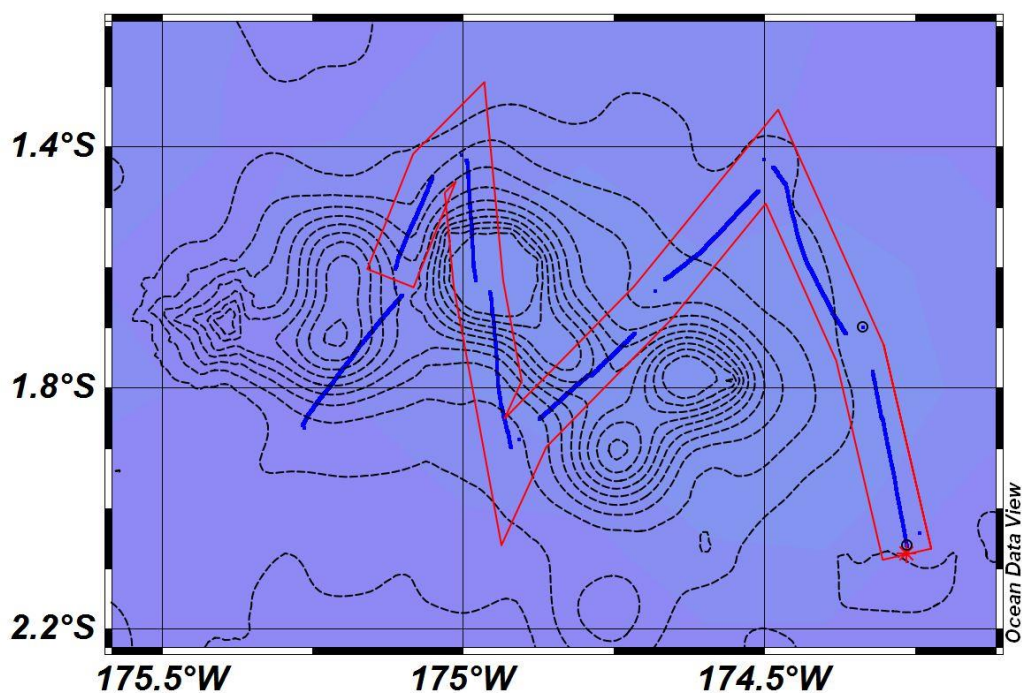


**Figure 15.** Depiction of tows completed during Towfin RBR CTD deployments. The seven sections within the highlighted area were analyzed for Chl a data.

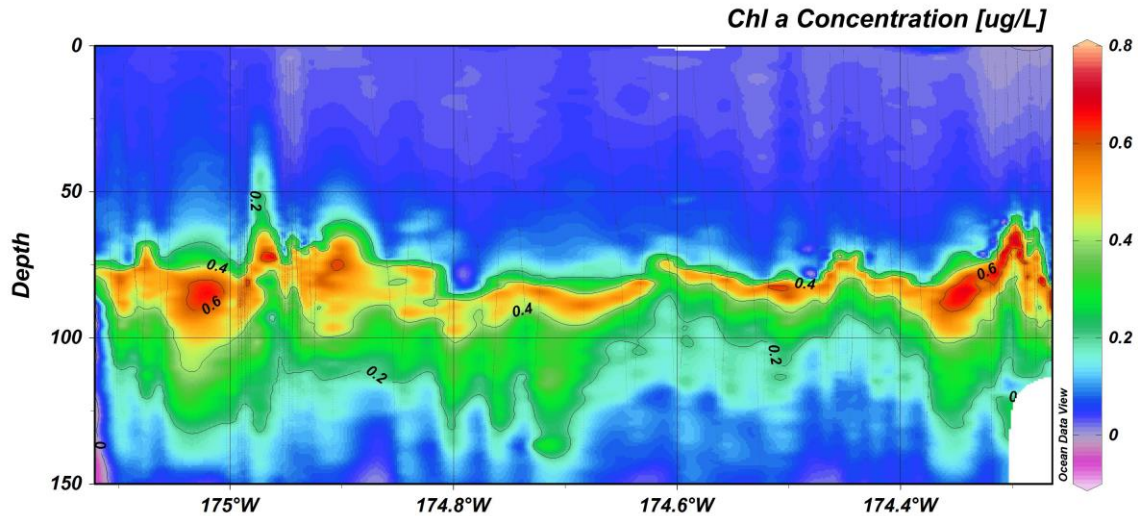


**Figure 16.** Grid plot of Chl a Concentration adapted from Towfin flow through flourometer data. Converted measurements are in ug/L.

#### Zooplankton:

Zooplankton densities for NT samples collected at each of the 8 Winslow Reef sites ranged from  $0.00325 \text{ mL/m}^2$  to  $0.01935 \text{ mL/m}^2$  while those for the shallow and deep TT samples ranged from  $0.00784 \text{ mL/m}^3$  to  $0.03232 \text{ mL/m}^3$  and  $0.00813 \text{ mL/m}^3$  to  $0.03336 \text{ mL/m}^3$ , respectively. Mean densities collected via the NT, shallow TT and deep TT deployments across all 8 sample sites were  $0.00726 \text{ mL/m}^2$ ,  $0.00813 \text{ mL/m}^3$ ,  $0.01962 \text{ mL/m}^3$  respectively (Figure 17). The highest zooplankton densities observed across all NT, shallow TT and deep TT deployment sample sites occurred at site numbers 4, 2 and 1, respectively while the diversity index values occurred at sites 8, 7 and 3, respectively (Figure 18).

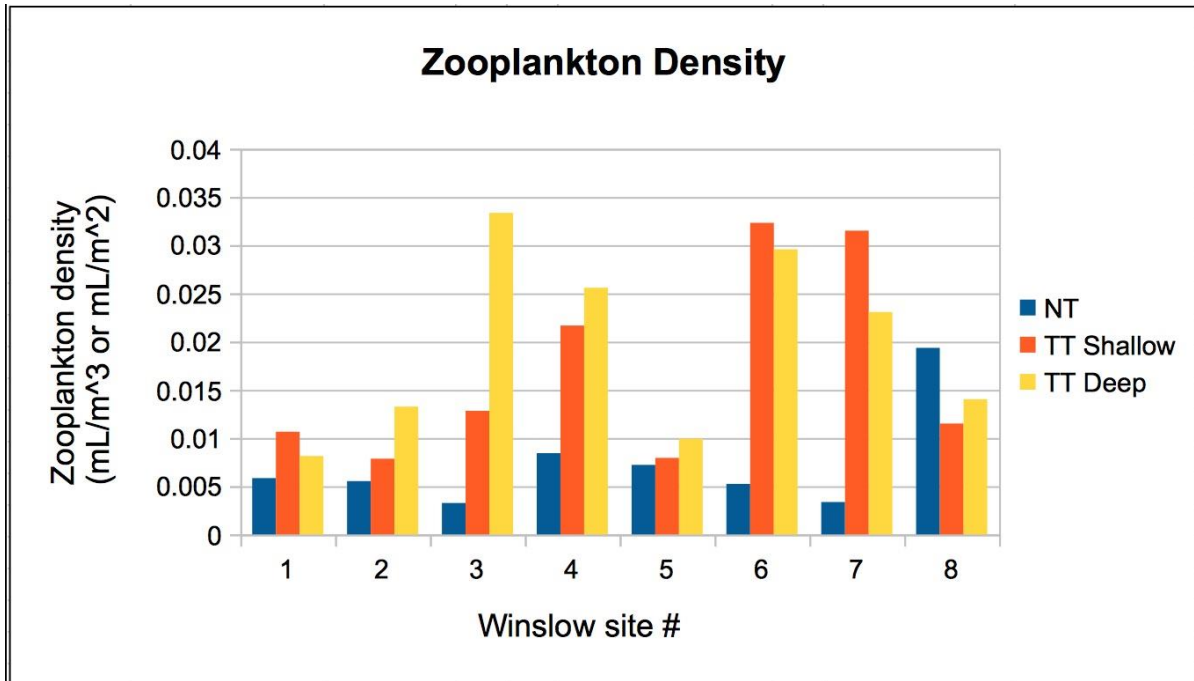


**Figure 17.** Zooplankton density results from shallow TT, deep TT and NT deployments at eight sample sites in Winslow Reef. NT median tow depth = 0m (density measured in mL/m<sup>2</sup>), shallow TT median tow depth = 25m (density measured in mL/m<sup>3</sup>), deep TT median tow depth = 50m (density measured in mL/m<sup>3</sup>).

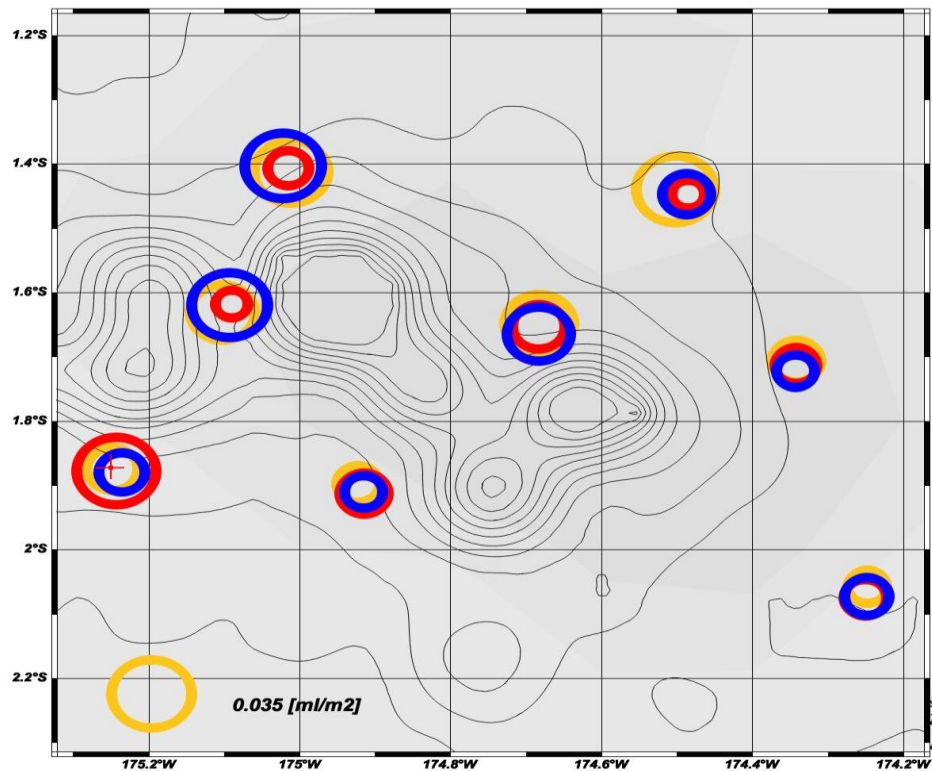


**Figure 18.** Zooplankton density results from deployments of NT (red), shallow TT (blue) and deep TT (yellow) at eight sample sites plotted against a bathymetric map of the Winslow Reef area. Circle size indicates magnitude of values and sample site numbers (1-8) occur in order from right to left. NT median tow depth = 0m (density measured in mL/m<sup>2</sup>), TT Shallow median tow depth = 25m (density measured in mL/m<sup>3</sup>), TT Deep median tow depth = 50m (density measured in mL/m<sup>3</sup>). Zooplankton density calculated for results from all three plankton tow nets. Red = neuston tow (0 m median tow depth), blue = Tucker trawl shallow tow (25m median tow depth), yellow = tucker trawl deep tow (50m median tow depth).

Shannon Weiner Diversity Index values for the zooplankton samples collected by the NT, shallow TT and deep TT deployments at each of the 8 Winslow Reef sites ranged from 0.0485 to 0.5424 (mean = 0.2359), 0.3980 and 0.7474 (mean = 0.5692), and 0.3565 to 0.7305 (mean = 0.5458), respectively (Figure 19). The highest diversity index values observed across all NT, shallow TT and deep TT deployment sample sites occurred at site numbers 5, 6 and 2, respectively while the diversity index values occurred at sites 4, 8 and 1, respectively (Figure 20).

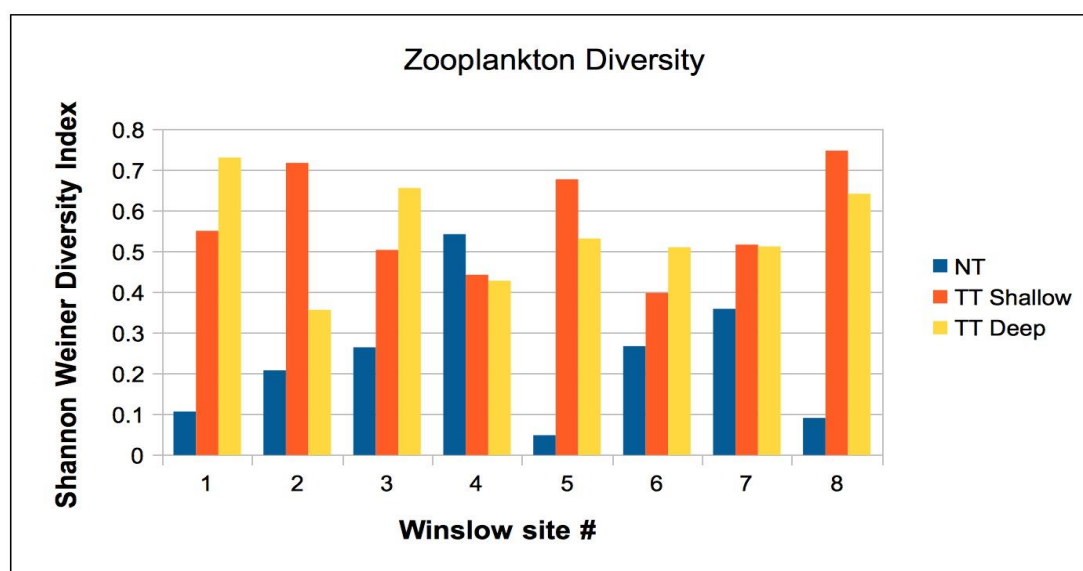


**Figure 19.** Shannon Weiner Diversity Index values for zooplankton samples collected from shallow TT, deep TT and NT deployments at eight sample sites in Winslow Reef. NT median tow depth = 0m, shallow TT median tow depth = 25m, deep TT median tow depth = 50m.



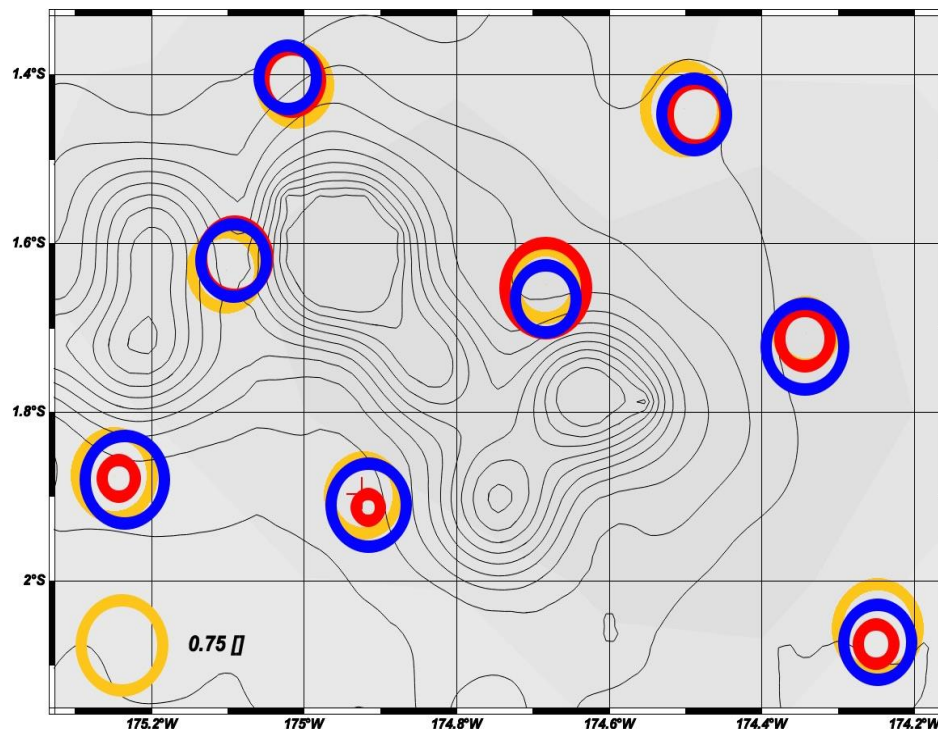


**Figure 20.** Shannon Weiner Index values for zooplankton samples collected by NT (red), shallow TT (blue) and deep TT (yellow) deployments at eight sample sites plotted against a bathymetric map of the Winslow Reef area. Circle size indicates magnitude of values and sample site numbers (1-8) occur in order from right to left. NT median tow depth = 0m, TT Shallow median tow depth = 25m, TT Deep median tow depth = 50m.

## Discussion:

### Currents:

Similar to how a rock in a stream interrupts the flow and creates disturbances, the seamount creates turbulence has the potential to interfere with both physical and biological parameters. Within the waters of PIPA, currents are predominantly influenced by three major patterns: the westward-flowing Equatorial Current, the south equatorial branch of the South Equatorial Current and the eastward-flowing equatorial counter-current. These currents can create some amount of mixing and disturbance on their own over Open Ocean but the seamounts within PIPA could potentially create greater disturbances than natural currents. If these seamounts do provide greater mixing then the potential for biological activity and hotspots is also greater.

What we found around Winslow reef is that there seems to be varying forms of disturbance at various depths. At around 50m, as illustrated in Figure 2, there seems to be some amount of deflection around the upper peaks of the seamounts. At 100m (Figure 3) there still seems to be deflection, but there also seems to be some circulation in the southern portions of the mount. As well, the deep channels seem to be beginning to show an influence on the currents by

providing some degree of venturi effect. This becomes more evident at 150m (Figure 4) where the channels seem to be helping the flow accelerate towards the south side. At 200m (Figure 5) the currents seem to change direction as well as weaken and become less consistent. All in all, this seems to imply that the seamounts definitely do create disturbances although the nature and method behind this is not obvious.

Some issues with our data and possible improvements to our methods revolve primarily around gathering more data. Our current data was gathered up to a depth of 600m, and only the first 200m were analyzed; yet the channels between peaks are towards 3000m deep and the sea floor is nearly 5000m. All together this means that we are only scratching the surface of what the currents are doing, and there are potentially deep-sea currents that are coming into play. As well, the surrounding waters currents could prove to show us how the currents approach Winslow and therefore how things are being disturbed. Finally, if our transects covered more of the seamount we would be able to tell a bit more about how deflection is occurring as well as get a better idea of the true depths and topography of the seamounts, as the current topography is likely to be inaccurate because it is based solely off of satellite information and we have already found flaws (such as needing to adjust the peak of the main reef from 2m below the surface to 20m).

### Salinity:

The salinity profile of the water column gives key insights to the behavior of the mixed layer, an important zone for biological processes where the water is well mixed allowing for a consistent temperature and salinity. The mixed layer is incredibly important for biological processes as mixing in the water column can also draw higher nutrient waters from depth to more photo productive zones (i.e. closer to the surface) allowing for greater productivity. Typically, the mixed layer resides approximately in the first 100m of the water column, however from figures 6 through 9 it is evident that the mix layer around Winslow Reef resides approximately between 48m and 70m. The relative shallow depth of the mix layer and the range in depth is indicative that the presence of Winslow is disrupting the mix layer.

Following the isohaline line of 34.75, the boundary of the mixed layer, it is evident that there are seemingly sporadic oscillations in this boundary across Winslow. The most notable and largest oscillations occur on the Eastern side of Winslow, with a range between 48 and 70m as made evident by figure 6. Following the transect made by our CTD tow and CTD deployments, it would appear that even though the depth of the 34.75 isohaline line continuously oscillates with clear local maxima and minima, the mean depth of this contour generally decreases from South to North. The relatively shallow and oscillating mix layer around Winslow would indicate the seamount is interfering with horizontal currents in the water column. The mean decrease in the depth of the mix layer boundary from South to North is most likely due to the North to South currents funneling between the seamounts, creating an upwelling current in its wake. There seems to be a correlation between shallower 34.75 isohaline line in the South compared to the North with the increase in surface currents in the South compared to the North. This behavior would indicate upwelling in the Southern region of the seamount.

Alternatively the mean decrease in the depth of the mix layer boundary from South to North may be a result of upwelling generated by another body of moving water. Below the mixed layer and up to around 200m, there is a zone of high salinity. This body of high salinity water is a result of processes occurring far from Winslow, namely in the sub-tropical convergence zone in the south Pacific. Due to Hadley convection cells, a lot of evaporation

occurs in the sub-tropical convergence zone creating a high salinity body of water. As the equatorial waters are zones of divergence, these waters are much less salty, thus a salinity gradient is formed. As with any gradient in a fluid, the high salinity water will move from the convergence zone towards the equator, slowly dispersing and sub-ducting, as it is denser than the lower salinity water it is moving towards. As this body of water moves across a seamount, it becomes perturbed similarly to the local currents become turbulent around Winslow. This body of salty water is moving from South to North, thus it is plausible that this water is being perturbed and kicked up to a shallower depth by Winslow. This would explain the shallower mean depth of the mix layer in the South of Winslow compared to the North.

#### Chlorophyll a:

Production is the total mass of organic matter that is created in an ecosystem and productivity is the rate at which biomass increases in an area per unit of time. Productivity is measured by the combination of primary productivity, the rate at which biomass is produced by autotrophs, and secondary productivity, the rate at which biomass is produced by heterotrophs (Allaby, 2010). As a prominent feature of Pacific Ocean bathymetry, seamounts are an important aspect to consider when looking at productivity of the oceans. As shown by Morato et al. (2010a), seamounts have the potential to be hotspots of biomass and productivity. As hotspots, identified and protected seamounts have the potential to conserve species biodiversity as well as facilitate better fisheries management (Morato et al., 2010a; Myers et al. 2000). This lends potential importance and use to these findings surrounding Chl a concentrations around Winslow Reef. Chl a concentrations were used as a proxy for primary productivity values in the areas measured.

A high concentration occurred on the upstream side of the seamounts, presumably before the turbulence effects caused by these structures had an effect on current flow. As measurements were taken in more westward longitudes, Chl a concentrations of greater than .2ug/L were seen to cover a larger, deeper section of depth (~75m-125m) as opposed to the higher concentrated, but more compressed measurements in the easternmost longitude measurements (~60-100m) (Figure 16). This deepening and greater spread of Chl a concentrations may be due to the currents, which flow in a generally north-east to south west direction. The concentration of Chl a measured around seamount stations (stations 5 and 6; Figure 11) falls between 50 and 100m (Figure 12; Figure 13). This may be due to the increased flow of the currents being deflected out of the deep channels of the seamounts at 50 and 100m (Figure 2; Figure 3). An increased spread of higher Chl a concentrations on the downstream side of the seamounts, as well high concentrations pushed to locations by deflected currents supports visible effects of the Island Mass Effect.

There were some complications and potential factors of error. The Fluorometer was not functional during the eighth towfin tow deployment (Figure 15). This is a complication due to the fact that a large section of the downstream side of the seamount area was unmeasured except by a single station. There is some error in the conversion of V data to ug/L, with a linear regression equation and an  $r^2$  value of .953747. One other possible problem with the presented data is that discrete measurements were only taken at 8 stations, at 6 depths down to 125m. While this is a considerable amount of information, it is still necessary for a large amount of extrapolation when constructing grid plots.

### Zooplankton:

Comparisons of the current pattern profiles at 50m and 100m depths (Figures 2 and 3) suggest that the movement of water masses at the depths traversed by the TT during deep tows would contribute towards higher zooplankton densities at the southwestern corner of the Winslow Reef area while water masses at the depths traversed by the TT during shallow tows would contribute towards higher zooplankton densities towards the west. Zooplankton density values did reflect these expected trends to some extent. Although it was not possible to render current pattern profiles at the sea surface, the larger density values recorded for the NT samples collected at the westernmost sample sites would have been expected to occur if the disturbance of water flows as a result of the seamounts contributed the general upwards movement of those masses. Zooplankton diversity values, on the other hand, did not show any identifiable patterns that could be correlated with current movements in Winslow Reef.

### Final notes:

Winslow Reef, one of the prominent seamount areas within the Phoenix Island Protected Areas shows characteristics related to the IME. Whether these characteristics are constant for Winslow, and whether Winslow is representative of other PIPA seamounts is unknown. However, it is important to begin to consider the effect seamounts such as these may have on current flow and productivity and diversity levels on the oceans. Further studies around Winslow and other such seamounts will be the vital next step in understanding more about the dynamics of ocean environments.

One thing of note is that the trends for this year suggest that an El Nino Southern Oscillation event is occurring. This has potential effects on the interpretation of our data. The changes that occur in the Pacific due to ENSO are considerable, and Winslow Reef is located in the Central Pacific, very close to the equator. Looking at seamounts, particularly Winslow, during ENSO years and non-ENSO years will be an important step in fully understanding seamount ecosystem function and the IME associated with seamounts.

### **Acknowledgments:**

Thanks to Jan and the crew of S-261 for helping us gather this data and complete our voyage!

## References:

- Allaby, Michael. *A Dictionary of Ecology*. Oxford University Press, 2010. Web.
- Arar, E.J, and G.B. Collons. 1997. Method 445.0: In *vitro* Determination of Chlorophyll a and Phaeophytin a in Marine and Freshwater Algae by Fluorescence (rev. 1.2). National Exposure Research Laboratory: US Environmental Protection Agency.
- Parsons T., Maita Y., and Lalli C. 1989. *A Manual of Chemical and Biological Methods for Seawater Analysis*. Pergamon Press, Inc.: Elmsford, NY.
- Elliot, J., Patterson, M., & Gleiber, M. (2012). Detecting 'Island Mass Effect' Through Remote Sensing. *Proceedings of the 12th International Coral Reefs Symposium*.
- Martinez, E., & Maamaatuaiahutapu, K. (2004). Island mass effect in the Marquesas Islands: Time Variation. *Geophysical Research Letters*, 31. doi:10.1029/2004GL020682
- Messie, M., Radenac, M., Lefevre, J., & Marchesiello, P. (2006). Chlorophyll bloom in the western Pacific at the end of the 1997 - 1998 El Nino: The role of the Kiribati Islands. *Geophysical Research Letters*, 33. doi:10.1029/2006GL026033
- Bakun, Andrew. "Local retention of planktonic early life stages in tropical reef/bank demersal systems: The role of vertically-structured hydrodynamic processes." *IOC/FAO Workshop on Recruitment in Tropical Coastal Demersal Communities. Ciudad del Carmen, Campeche, Mexico. Report*. Vol. 40. 1986.
- Pitcher, Tony J., Telmo Morato, Paul J.B Hart, Malcom R. Clark, Nigel Haggan, and Ricardo S. Santos. *Seamounts: Ecology, Fisheries & Conservation*. Oxford: Blackwell Publishing, 2007. Print. Ser. 12.
- Boehlert, G. W., & Genin, A. (1987). A review of the effects of seamounts on biological processes. *Seamounts, islands and atolls*, 43, 319-334.
- Pennington, J. Timothy; Mahoney, Kevin L.; Kuwahara, Victor S.; Kolber, Dorota D.; Calienes, Ruth; Chavez, Francisco P. "Primary production in the eastern tropical Pacific: A review." *Progress in Oceanography*, Vol. 69 (2006): 285–317. Web.
- Gilmartin, Malvern, and Noelia Revelante. "The 'island mass' effect on the phytoplankton and primary production of the Hawaiian Islands." *Journal of Experimental Marine Biology and Ecology* 16.2 (1974): 181-204.
- Hernández-León, Santiago. "Accumulation of mesozooplankton in a wake area as a causative mechanism of the "island-mass effect". *Marine Biology* 109.1 (1991): 141-147.
- Morato, Telmo, Cathy Bulman, and Tony J. Pitcher. "Modelled effects of primary and secondary

production enhancement by seamounts on local fish stocks." *Deep Sea Research Part II: Topical Studies in Oceanography* 56.25 (2009): 2713-2719.

Morato, Telmo; Simon D. Hoyle, Valerie Allain, Nicol, Simon J. Nicol. "Seamounts are hotspots of pelagic biodiversity in the open ocean." *Proceedings of the National Academy of Sciences* 107.21 (2010a): 9707-9711.

Morato, Telmo; Simon D. Hoyle; Valerie Allain; Nicol, Simon J. "Tuna Longline Fishing Around West and Central Pacific Seamounts." *PLoS ONE*, (2010b): Vol. 5, Issue 12, 1-7. Web.